How can solar panels collectors enhance energy efficiency? Utilization of the novel optimization techniques

Kairat A. Kuterbekov[1], Asset M. Kabyshev[1], Kenzhebatyr Zh. Bekmyrza[1], Marzhan M. Kubenova[1,*] and Abebe T. Ayalew[2,*,†]

[1]Faculty of Physics and Technical Science, L.N. Gumilyov Eurasian National University, 010008, Satpayev st. 2, Astana, Kazakhstan; [2]Faculty of Hydraulic and Water Resources Engineering, Arba Minch University, P.O. Box 21, Arba Minch 4400, Ethiopia

Abstract

Solar energy, which is widely acknowledged for its economic feasibility and sustainable nature, functions as a critical substitute for finite fossil fuels, effectively alleviating ecological consequences. The purpose of this study is to investigate the implementation of solar collectors as a means of harnessing the ample and unaltered solar radiation in Iran, specifically in locations situated within the solar belt. The incorporation of solar energy not only aids in the expansion of energy sources through diversification but also mitigates the rising expenses linked to fossil fuels. The preservation of natural resources, coupled with limited renewable energy options, further accentuates the importance of solar energy. The optimization of solar panel collector angles in photovoltaic systems assumes paramount importance for maximizing energy efficiency. This study, conducted in Yazd, Iran, utilized innovative mathematical and particle swarm optimization (PSO) models to assess ideal inclination angles. Results indicate peak solar energy absorption during June and July, contrasting with minimal absorption in January. The Klein model prescribes inclination angles based on γ values, while the PSO algorithm determines optimal slope and azimuth angles across various periods. Significant enhancements in energy generation, ranging from 23.24 to 25.02% across optimization models, were observed compared to a horizontal surface. These findings underscore the imperative of optimizing solar panel placement in urban settings to augment energy generation. Utilizing the optimal orientation for the photovoltaic power supply system can result in an annual reduction of 1169.6 kg of CO_2 emissions in the building, emphasizing the positive environmental impact achievable through strategic solar panel configurations.

Keywords: solar panel; collector; novel optimization; energy efficiency; electricity production; CO2 emission

*Corresponding author.
kubenova.m@yandex.kz;
abebe.temesgen@amu.edu.et

Received 1 December 2023; revised 15 February 2024; accepted 15 March 2024

1. Introduction

The ongoing concern pertains to the depletion of fossil energy sources [1, 2]. The increasing worldwide need for energy consumption, combined with the decreasing availability of fossil fuels, requires the adoption and enlargement of innovative methods to reduce energy consumption [3–7]. In addition, the sun has a significant effect on human health and can prevent a variety of diseases [8–10]. Utilizing fossil fuel alternatives, such as solar energy, in vehicles, buildings and other areas can effectively decrease the release of environmental pollutants, specifically CO_2 [11–15].

The utilization of novel energy systems as a sustainable and cost-effective power source has been a longstanding practice among human beings, despite its detrimental impact on the environment [16–20]. The utilization of solar collectors has enabled the increased utilization of an abundant, unaltered and cost-free energy source, thereby reducing the reliance on fossil fuels [21–24]. Iran is located within the solar belt and

[†], https://orcid.org/0009-0006-3679-0907

https://doi.org/10.1093/ijlct/ctae048

is acknowledged as one of the countries that experiences a significant influx of solar radiation annually [25, 26]. Based on the evaluations, it seems that the general populace has exhibited a favorable response to it. The utilization of multiple energy sources is crucial in the event of unforeseen incidents [27, 28]. Therefore, the adoption of solar energy serves as an additional incentive to do so. The significance of solar energy for the island is multifaceted, with one of the reasons being its natural resource scarcity and the need to safeguard them for posterity [29, 30]. Another factor contributing to the adoption of alternative energy sources is the comparatively elevated expenses associated with the utilization of fossil fuels, which are on the rise [31–33].

Solar energy has emerged as a crucial player in addressing global energy needs, offering a sustainable and environmentally friendly alternative to conventional fossil fuels [34, 35]. Solar radiation is the primary source of solar energy that the Earth receives. The quantity of radiant energy emitted by the sun is contingent upon two primary factors: The temporal dimensions under consideration are the hour, day and season and the location is determined by the geographical latitude [36–38]. The sun's perpetual movement across the sky and its daily varying trajectory necessitate directional adjustments to optimize the reception of radiant energy, owing to the differing radiation angles in each region [39, 40]. The efficient utilization of solar power is contingent upon the proper adjustment and optimization of solar collectors within photovoltaic systems [41, 42]. Solar collectors play a pivotal role in harnessing sunlight for energy conversion [43]. Proper adjustments, including inclination angles and azimuth orientation, significantly influence the amount of solar radiation captured. Studies indicate that precise alignment with the sun's path enhances energy absorption, ensuring maximum utilization of available solar resources [44]. The optimization of solar collector adjustments contributes to increased energy yield, making it a crucial aspect of photovoltaic system design.

The efficiency of photovoltaic systems is intrinsically linked to the alignment of solar collectors. Appropriate adjustments mitigate energy losses caused by suboptimal orientation, shading or misalignment. By fine-tuning these parameters, system efficiency is optimized, resulting in higher energy output and improved overall performance. Solar collector adjustments influence the economic feasibility of photovoltaic installations. By maximizing energy production, proper alignment enhances the return on investment for solar projects. The reduction in operational costs and increased energy output contribute to the long-term economic viability of solar energy systems, making them attractive options for both residential and commercial applications.

Benghanem [45] determined the optimal angle for maximizing received energy during a shot test conducted in Madinah. The researcher arrived at the determination that the optimal angle of inclination for a given year is nearly equivalent to the geographic width of the area. Additionally, the energy yield resulting from a monthly slope is eight times greater than that of an annual slope. Lahjouji and Darhmaoui [46] used a mathematical model for the calculation of radiation on a sloping surface in Morocco. The researchers acquired the seasonal inclination of 5.21° during spring, 6° in summer, 2.51° in autumn and 8.62 degrees in winter. They proposed that the yearly inclination is equivalent to the geographic latitude. According to Lubitz [47] findings, under favorable weather conditions and for geographic latitudes of 65°, the annual ideal slope angle is roughly 0.9 times the geographical latitude of the location. In certain regions, maintaining a consistent slope angle throughout the year may be optimal, while in other cases, altering the slope angle periodically can enhance operational efficiency. According to Moghadam *et al*. [48] research conducted in the urban areas of Zahedan and Bandar Abbas, adjusting the optimal angle of inclination twice a year results in an 8% increase in energy usage compared to maintaining a constant system throughout the year. The variable azimuth angle has been obtained. Lv *et al*. [49] introduced a mathematical framework for determining the optimal orientation and inclination angle of solar collectors in Lhasa throughout the heating season. A discrepancy of 5° exists between the optimal orientations determined by total solar radiation and those determined by effective solar heat collection. Alharbi *et al*. [50] present a model designed to integrate models of total irradiance with the solar panels temperature model. The purpose of this integration is to determine the optimal solar collector module installation parameters throughout the year. In order to optimize energy output, the study analyzed the integration between installation parameters and annual average solar energy. Al-Ghussain *et al*. [51] employed ground-level meteoro-solar data to assess and compare different models used for calculating diffuse irradiance. The researchers also analyze the influence of operating temperature, wind speed and dust deposition on energy generation. Additionally, they examine the most favorable tilt and azimuth angles of the panels in three cities located in Egypt, Tunisia and Jordan. The results suggest that the isotropic model generated energy production estimates that were 1.5% higher than those of the anisotropic model in the summer season. Yoon *et al.* [52] propose a mathematical approach to optimize the positioning of solar panels on multi-apartment buildings. Presently, the use of photovoltaic power generating has progressively emerged as a highly efficient approach. Although this technique does not cause environmental pollution, its efficiency in generating power is quite low.

To achieve optimal solar energy efficiency in a photovoltaic system, solar panels must be optimally placed and collector angles calibrated in respect to sunlight. Undoubtedly, understanding the ideal location of solar panel collectors at right angles has the potential to improve energy efficiency. As a result, verifying such information can be extremely useful for stakeholders participating in decision-making processes. The purpose of this study is to determine the optimal angle of solar panel collectors in a photovoltaic system for the Yazd urban region in Iran. This study focuses on the creation of an optimization model to address the difficulty of establishing the best angle of orientation for solar panel collectors during different seasons of the year. The goal is to improve the efficiency and effectiveness of solar energy extraction. In addition, a comparative analysis was performed to compare the results of several optimization strategies to the current model. The evaluation uses a mathematical model and a particle swarm optimization (PSO) optimization methodology. Meanwhile, an evaluation has been made of the annual reduction in CO_2 emissions in the atmosphere caused by the installation of a photovoltaic system in a typical building.

2. Mathematical optimization model

The analysis of data pertaining to the received energy on the horizontal surface (H) for modeling the sun radiation of Yazd was conducted over the period spanning from 2012 to 2022. The net coefficient of air can be determined by utilizing mathematical relationships through the process of data averaging, with the ultimate goal of ascertaining the quantity in energy evaluation. Mathematical models have been developed to analyze the transmission of energy to a horizontal surface using radiation energy data (Eq. 1).

$$H_T = H_b + H_d + H_r, \tag{1}$$

where H_b is the total direct radiation, H_d is the transmitted radiation and H_r is the reflected radiation.

One of the mathematical models for evaluating the H_T is Liu and Jordan method [53]. Using this method, the amount of monthly average radiation on the sloping surface is calculated as Eq. 2:

$$H_T = H\left(1 - \frac{H_d}{H}\right) R_b + H_d\left(\frac{1+\cos\beta}{2}\right) + H\rho\left(\frac{1-\cos\beta}{2}\right), \tag{2}$$

where β is the slope angle, ρ is the ground reflection coefficient and H is the level of radiation on the horizontal surface, and R_b is the ratio of the average amount of direct radiation on the inclined surface to the average amount of direct radiation on the flat surface (see Eqs. 3 and 4).

$$R_b = \frac{\cos(\varphi-\beta)\cos\delta\sin\omega_s + \left(\frac{\pi}{180}\right)\omega_s\sin(\varphi-\beta)\sin\delta}{\cos\varphi\cos\delta\sin\omega_s + \left(\frac{\pi}{180}\right)\omega_s\sin\varphi\sin\delta}, \tag{3}$$

$$\begin{gathered}\omega_s = \cos^{-1}(-\tan\varphi\cdot\tan\delta)\\ \omega_s = \min\begin{bmatrix}\cos^{-1}(-\tan\varphi\cdot\tan\delta)\\ \cos^{-1}(-\tan(\varphi-\beta)\cdot\tan\delta)\end{bmatrix}.\end{gathered} \tag{4}$$

Eqs. 3 and 4 are for the Northern Hemisphere in the context of their respective associations. The aforementioned equation involves the utilization of various parameters, namely the geographic latitude of the location denoted by φ, the angle of the earth's axis deviation during the relevant time represented by δ (Eq. 5). The angle of sunrise on the horizontal plane indicated by ω_s, and the angle of sunrise on the plane of the horizon expressed in degrees as ω_s (Eq. 5).

$$\delta = 23.5\sin\left[360\times\frac{n}{365}\right]. \tag{5}$$

The clear air coefficient (K_{th}) is a mathematical representation of the proportion between the overall radiation received on a horizontal plane and the radiation received on the same plane in the absence of the Earth's atmosphere, as denoted by Eq. 6.

$$K_{th} = \frac{H}{H_0}. \tag{6}$$

Eq. 7 provides a means for extracting trans atmospheric radiation H_0.

$$\mathrm{H}_0 = \frac{I_{sc}}{\pi}\left(1 + 0.033\cos\frac{360n}{365}\right) \times\left[\cos\varphi\cos\delta\sin\omega_s + \frac{\pi\omega_s}{180}\sin\varphi\sin\delta\right]. \tag{7}$$

I_{SC} is a solar constant whose value is 1367 W/m². Several mathematical models exist to estimate the ratio of scattered radiation to total radiation (K_{dh}). For the Middle East region, the Orgill and Hollands [54] model is deemed to be more appropriate. This model takes into account the proportion of scattered radiation in relation to the overall radiation. Equation 8 yields the net coefficient of air.

$$\begin{cases} K_{dh} = 1.557 - 1.84\,K_{th} & 0.35\langle\, K_{th}\langle 0.75\\ K_{dh} = 1 - 0.249\,K_{th} & K_{th}\langle 0.35\\ K_{dh} = 0.177 & K_{th}\rangle\, 0.75\end{cases}. \tag{8}$$

Klein has proposed a methodology known as the K_T model, which incorporates an assessment of the impact of azimuth angles. The relevant mathematical expressions are denoted as Eqs. 9 to 18 [55].

$$H_T = \mathrm{HD} + H_d\left(\frac{1+\cos\beta}{2}\right) + H\rho_g\left(\frac{1-\cos\beta}{2}\right); \tag{9}$$

$$D = \begin{cases}\max(0, G(\omega_{ss},\omega_{sr})\} & \text{if } \omega_{ss}\geq\omega_{sr}\\ \max(0,[G(\omega_{ss},-\omega_s) + G(\omega_s,\omega_{sr})] & \text{if } \omega_{sr}\succ\omega_{ss}\end{cases}; \tag{10}$$

$$\begin{aligned} G(\omega_1,\omega_2) = \frac{1}{2d}\Bigg[&\left(\frac{bA}{2} - a'B\right)(\omega_1-\omega_2)\frac{\pi}{180} + \left(a'A - bB\right)\\ &\cdot(\sin\omega_1 - \sin\omega_2) - a'C(\cos\omega_1 - \cos\omega_2)\\ &+\left(\frac{bA}{2}\right)(\cos\omega_1\sin\omega_1 - \cos\omega_2\sin\omega_2)\\ &+\left(\frac{bC}{2}\right)\left(\sin^2\omega_1 - \sin^2\omega_2\right)\Bigg]; \end{aligned} \tag{11}$$

where,

$$a' = a - \frac{H_d}{H}; \tag{12}$$

$$a = 0.409 + 0.5016 \sin(\omega_s - 60); \tag{13}$$

$$b = 0.6609 - 0.4767 \sin(\omega_s - 60) \;. \tag{14}$$

The angles of sunrise ω_{sr} and sunset ω_{ss} are calculated based on Eqs. 15–18:

$$|\omega_{sr}| = \min\left[\omega_s, \cos^{-1}\frac{AB + C\sqrt{A^2 - B^2 + C^2}}{A^2 + C^2}\right]; \tag{15}$$

$$\omega_{sr} = \left\{ \begin{array}{l} -|\omega_{sr}| \text{ if } (A > 0 \text{ and } B > 0) \text{ or } (A \geq B) \\ +|\omega_{sr}| \text{ otherwise} \end{array} \right]; \tag{16}$$

$$|\omega_{ss}| = \min\left[\omega_s, \cos^{-1}\frac{AB - C\sqrt{A^2 - B^2 + C^2}}{A^2 + C^2}\right]; \tag{17}$$

$$\omega_{ss} = \left\{ \begin{array}{l} -|\omega_{ss}| \; \textit{if} \; (A > 0 \text{ and } B > 0) \text{ or } (A \geq B) \\ +|\omega_{ss}| \text{ otherwise} \end{array} \right. , \tag{18}$$

where,

$$A = \cos\beta + \tan\phi\cos\gamma\sin\beta \tag{19}$$

$$B = \cos\omega_s\cos\beta + \tan\delta\cos\gamma\sin\beta \tag{20}$$

$$C = \frac{\sin\beta\sin\gamma}{\cos\phi} \;. \tag{21}$$

The mathematical expressions denoted as Eq. 9–Eq. 18 are commonly referred to as the K_T model. The present model employs Eqs. 22 and 23 for the computation of H_d.

$$\text{for } \omega_S \leq 81.4^{\circ}, ; \tag{22}$$

$$\frac{H_d}{H} = \left\{ \begin{array}{ll} 1 - 0.2727K_T + 2.4495K_T^z - 11.9514K_T^x + 9.3879K_T^t & \text{for } K_T < 0.715 \\ 0.143 & \text{for } K_T \geq 0.715 \end{array} \right.$$

$$\text{for } \omega_S > 81.4^{\circ},$$

$$\frac{M_d}{N} = \left\{ \begin{array}{ll} 1 + 0.2832K_T + 2.5557K_T^4 - 0.8448K_T^* & \text{for } K_T < 0.715 \\ 0.175 & \text{for } K_T \geq 0.715 \end{array} \right. . \tag{23}$$

Given the variability of received energy standard deviation across different days of a month, it is imperative to ensure the accuracy and generalizability of the optimal angle derived from the Gaussian regression model and two controls for estimating the total radiation amount. It was utilized on a daily basis. The Gaussian model's parameters associated with the Eq. 24 are equivalent to the two parameters of the model linked to Eq. 25. The regression coefficients, denoted by a_1, a_2, and a_{11}, along with the day number of the year, represented by n, are included in the model.

$$H = a_1 \exp\left(-\left(\frac{n - a_2}{a_3}\right)^2\right), \tag{24}$$

$$\begin{array}{l} H = a_4n^3 + a_5n^2 + a_6n + a_7n \leq 182 \\ H = a_8n^3 + a_9n^2 + a_{10}n + a_{11}n > 182 \end{array} . \tag{25}$$

In order to assess the model's efficacy and conduct a statistical comparison between the actual and predicted data, the employment of the root mean square error (RMSE) and the mean absolute percentage of the error (MAPE) was undertaken, as described in Eqs. 26 and 27.

$$\text{MAPE} = \frac{1}{n}\sum_{j=1}^{n}\left|\frac{H_a - H_p}{H_a}\right| \times 100 \;, \tag{26}$$

$$\text{RMSE} = \sqrt{\frac{\sum_{j=1}^{n}\left(H_a - H_p\right)^2}{n}}, \tag{27}$$

where H_a is the actual radiation value and H_p is the predicted radiation value.

3. PSO

The concept of the interest-based particle community approach was initially developed to facilitate the graphical representation of the captivating and erratic flight patterns exhibited by avian species [56]. The spatial arrangement of particles is subject to alterations based on their individual encounters and those of their proximate counterparts. The position and velocity of particle *i* are designated by the following parameters:

$$\vec{x}_i(t+1) = \vec{v}_i(t+1) + \vec{x}_i(t), \tag{28}$$

$$\vec{v}_{i\vec{i}}(t+1) = \omega\vec{v}_i(t) + c_1r_1\left(P_{gbesti} - \vec{x}_i\right) + c_2r_2\left(G - \vec{x}_i\right). \tag{29}$$

The $\vec{x}_i(t)$ and $\vec{v}_i(t)$ are utilized to display the position and velocity of the i-th particle at a given time t. The variable ω represents inertia, while r_1 and r_2 are random numbers that fall within the range of (1 and 0). The acceleration coefficients, denoted as C_1 and C_2, are considered to be fixed and positive. P_{gbesti} represents the maximum spatial value attained by particle *i*, whereas G represents the maximum spatial value attained overall. The objective of this study was to determine the optimal panel angle for maximizing solar radiation. To achieve this, the radiation function was utilized as the merit function and the panel angle was considered as the optimization variable [57–59]. Figure 1 shows the flowchart of the PSO algorithm.

4. Results and discussion

4.1. Optimal angel prediction

To assess the viability of solar panel collectors in enhancing energy efficiency, our study leveraged data spanning a decade (2012–2022) procured from the Meteorological Organization, focusing

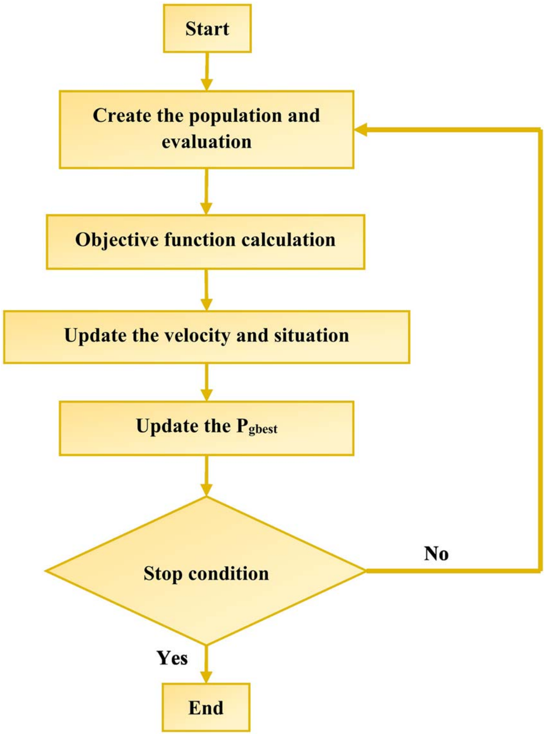

Figure 1. *PSO flowchart.*

Table 1. *The regression and two-control fitted model performance*

Model	Mean	Variance	RMSE	MAPE
Eq. 24	0.83	0.81	0.59	10.38
Eq. 25	0.87	0.68	0.51	8.11

on the urban locale of Yazd, Iran. Situated in a desert region at an elevation of 992 m above sea level (longitude 41.72°, latitude 27.51°), Yazd benefits from an arid climate, ensuring a consistent influx of sunlight throughout the year. The monthly average daily data on the horizontal surface, used as input for our models, aimed to capture the nuanced variations in solar radiation.

The importance of ground reflection in solar energy absorption was factored into our analysis, assuming a reflection coefficient of 0.2 (Figure 2a). Figure 2b visually presents the solar radiation energy received on a horizontal surface across different months in Yazd. Notably, June emerges as the peak month, witnessing the highest solar energy input at an impressive 28 150 kJ/m^2. Conversely, January exhibits the lowest solar energy input, recording a value of 13 152 kJ/m^2.

This detailed examination emphasizes the dynamic nature of solar energy availability, displaying the significant fluctuations that occur throughout the year. Understanding these variations becomes pivotal in identifying optimal angles for solar panels, particularly in the context of solar-powered systems catering to the energy demands of urban areas. Our findings underscore the importance of not only capturing peak solar months but also strategizing for periods of lower solar input to ensure a resilient and efficient solar energy system for Yazd.

In this study, we introduced and rigorously assessed two models: Gaussian models (Eq. 20) and regression models of the third and fourth orders (Eq. 21) for estimating annual radiation levels. The investigation delved into the fundamental importance of determining the ideal collector angle within the studied region to establish a robust framework for accurately approximating the quantity of radiation. The principles or values guiding these models' development were grounded in the overarching goal of improving solar panel efficiency.

Figure 3a and 3b present compelling insights into the performance of the Gaussian and two-control models by showcasing the frequency distribution of errors over the course of the year. The value of the error range for horizontal radiation estimation consistently falls within the range of −0.5 to 0.5 in more than 78% of days, indicating a high level of accuracy. Notably, the distribution of errors demonstrates a striking proximity to the normal distribution, underscoring the reliability and consistency of both models in estimating radiation levels.

The Gaussian model and two-control model exhibit robustness, capturing the dynamics of solar radiation variation throughout the year. These findings underscore the effectiveness of our proposed models in providing accurate estimates, contributing to the overarching goal of enhancing energy efficiency through optimal solar panel orientation. Moreover, the evaluation of error distributions over an annual cycle allows us to draw insightful conclusions about the models' performance under varying solar conditions. The consistency observed in error ranges emphasizes the reliability of our models across different periods, providing valuable information for practical applications in solar energy systems.

The statistical analysis conducted to evaluate the dependability of the Gaussian regression model and the fitted two-control model is summarized in Table 1. This analysis compares the anticipated radiation values with the observed values at a significance level of one percent. The table presents key performance metrics for both models.

The results indicate that both models perform well in capturing and predicting radiation values. Eq. 24 demonstrates a mean of 0.83, a variance of 0.81, a RMSE of 0.59 and MAPE of 10.38. Similarly, Eq. 25 exhibits a mean of 0.87, a variance of 0.68, an RMSE of 0.51 and a MAPE of 8.11. These metrics collectively attest to the reliability and accuracy of both models in estimating radiation levels.

As previously discussed, the calculation of radiation energy reaching an inclined surface relies on the radiation energy received on a horizontal surface. It is important to note that the negative values assigned to the tilt angle indicate that the collector is oriented toward the northern direction. Conversely, when the slope angle exhibits a negative sign, the collector is oriented toward the south. This statistical analysis not only reinforces the robustness of the Gaussian regression model and the fitted two-control model but also provides quantifiable metrics for their

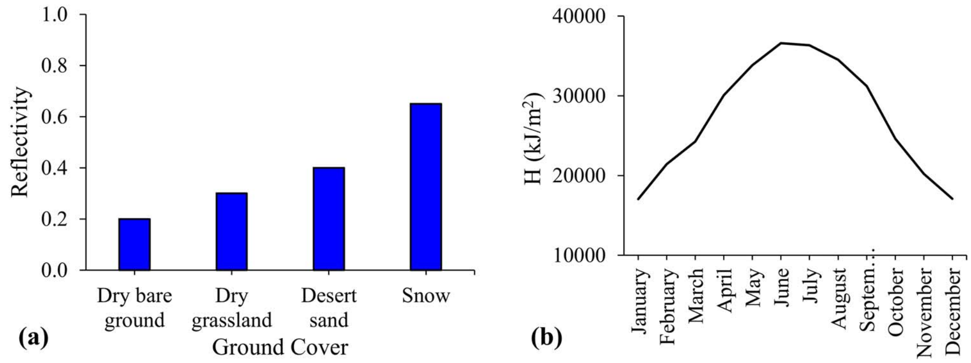

Figure 2. *(a) Reflectivity coefficient for different Ground cover [60] (b) Average daily total radiant energy per month for Yazd, Iran.*

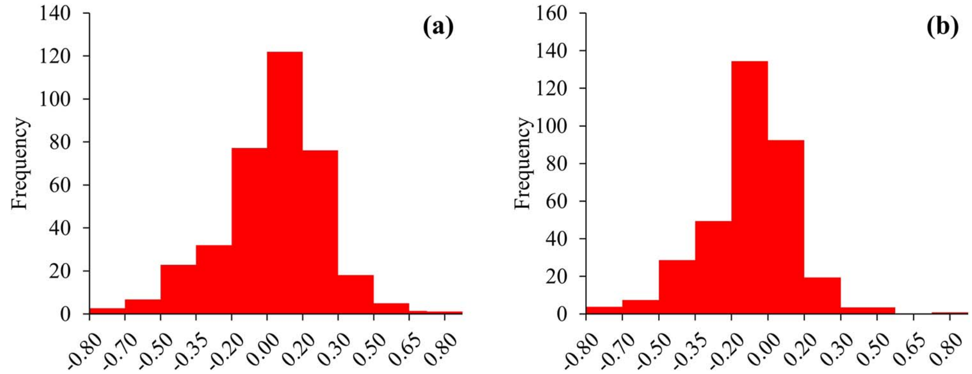

Figure 3. *(a) Frequency distribution of errors of the Gaussian model and (b) fitted two-rule model during the days of the year along with its normal diagram.*

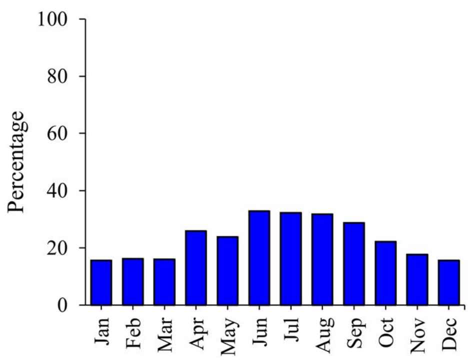

Figure 4. *The attain energy receive in different mouths by optimal angel using isotropic model.*

Table 2. *Comparison between present study and [61] for monthly values of optimal angle*

Month	Equation	$\beta_{opt\,(m)}$ [61]	$\beta_{opt\,(m)}$ (present study)
January	$\beta_{opt(m)} = 0.89\phi + 29$	57.38	55.11
February	$\beta_{opt(m)} = 0.97\phi + 17$	47.93	44.34
March	$\beta_{opt(m)} = \phi + 4$	35.89	29.82
April	$\beta_{opt(m)} = \phi$-10	21.89	17.84
May	$\beta_{opt(m)} = 0.93\phi$-24	5.66	3.88
June	$\beta_{opt(m)} = 0.87\phi$-34	-6.26	-7.09
July	$\beta_{opt(m)} = 0.89\phi$-30	-1.62	2.88
August	$\beta_{opt(m)} = 0.97\phi$-17	13.93	12.11
September	$\beta_{opt(m)} = \phi$-2	29.89	23.71
October	$\beta_{opt(m)} = \phi + 12$	43.89	42.41
November	$\beta_{opt(m)} = 0.93\phi + 25$	54.66	55.69
December	$\beta_{opt(m)} = 0.87\phi + 34$	61.74	59.12

performance. The low values of RMSE and MAPE underscore the models' ability to closely approximate observed radiation values, further validating their utility in practical applications within the context of solar energy systems.

Table 2 provides a comprehensive comparison of optimal tilt angles for solar panels between the present study and the Nijegorodov *et al*. [61] study. The equations determining these angles based on latitude (ϕ) for the northern hemisphere are highlighted in the second column. The third column displays the values derived by Nijegorodov *et al*. [61], while the fourth column presents the values obtained through the mathematical optimization technique in the present study.

The outcomes reveal a close alignment between the two approaches, with minimal disparities. These optimal tilt angles are crucial for maximizing solar panel efficiency and energy capture throughout the year in the specific geographic location of Yazd. This comparative analysis further substantiates the effectiveness

Table 3. *The optimal angle and average daily and monthly energy values attained by the solar panel surface determined by the monthly, seasonal, and annual optimal angles*

Month	β opt(m)average	H opt (m) (kJ/m^2)	β opt(s)average	H opt (s) (kJ/m^2)	β opt(y)average	H opt (y) (kJ/m^2)
January	54.31	18 851	47.14	18 910	25.15	18 255
February	43.24	20 643		20 233		20 916
March	27.67	24 166		24 352		24 138
April	15.84	25 522	5.59	25 942		25 492
May	2.98	28 134		27 919		26 689
June	-8.29	31 069		30 454		26 930
July	1.18	30 331	10.16	30 275		28 821
August	12.84	27 447		27 230		27 443
September	22.71	29 618		28 496		29 813
October	40.73	26 189	53.62	27 099		25 991
November	55.61	25 082		25 671		24 387
December	57.11	21 923		22 321		22 978

and reliability of the optimization technique proposed in this study.

Upon comparison, a minor discrepancy is observed between the optimal angles obtained through mathematical optimization and those derived by Nijegorodov *et al*. [61]. This discrepancy is attributed to the distinct mathematical approaches employed in both techniques and the functional trajectory of radiation energy values specific to the geographic region of Yazd.

Table 3 presents the optimal tilt angles and the corresponding radiation energy values on the slope surface for each month, season and the entire year. Notably, optimal angles exhibit negative values during May, June and July, indicating a tilt toward the northern direction, while positive values are observed in other months. Seasonal averages and an annual overview further provide insights into the dynamic nature of solar panel orientation requirements for optimal energy capture in the unique climatic conditions of Yazd.

It is evident from Figure 4 that the maximum solar energy intake occurs in June, reaching 30 331 kJ/m^2, while the minimum is recorded in January, with a value of 18 851 *kJ/m^2*. The seasonal optimization approach highlights these months as periods of peak and nadir in received radiation energy, with recorded values of 30 454 kJ/m^2 and 23 233 kJ/m^2, respectively. When optimizing the annual radiation energy intake, it is advisable to consider September and January, associated with the highest (29 813 kJ/m^2) and lowest (18 255 kJ/m^2) energy intake, respectively.

The average annual solar energy obtained using ideal angles for each month, season and the entire year exhibits a significant increase of 23.24% compared to energy obtained at the horizon's surface (Figure 4).

The isotropic model, applicable when γ equals zero, is contrasted with non-isotropic and optimization models in Figure 5, presenting radiation energy values for different inclinations of the steep side (γ). The Klein model specifies the use of values of ϕ, $\phi \pm 10$, $\phi \pm 20$ for the respective months of January and July. This analysis underscores the importance of considering optimal angles derived through mathematical optimization, particularly when aiming to enhance annual radiation energy intake. The diverse climatic conditions and geographical parameters of Yazd make the optimization models crucial for accurate solar panel orientation and, consequently, improved energy efficiency. According to the findings of Klein's model (Figure 5a), it has been observed that the energy receives the highest daily amount when the angle of inclination is $\phi + 20$ for $\gamma < 55$. Conversely, for $\gamma > 55$, the optimal angle of inclination is $\phi - 20$. According to Figure 5b, the outcomes indicate that the model demonstrates the maximum energy level for July when the slope angle is at $\phi - 20$ (Figure 5b).

The annual average solar energy quantities, acquired at optimal angles through the PSO algorithm, showcase a substantial increase of 24.47% compared to solar energy obtained at the surface of the horizon (Figure 6).

Figure 6a illustrates the outcomes of the PSO algorithm, indicating that in January, the highest energy yield is achieved at a slope angle of $\phi + 16$, with the optimal azimuth angle for maximizing energy throughout the year is equal to 78. Similarly, in June, the maximum energy is attained at a slope angle of $\phi - 23$, with the optimal azimuth angle being zero. The calculations consider optimal daily, monthly, seasonal and annual angles. The detailed results highlight that the energy intake throughout the year experiences a steady increase, averaging at 25.02% (Figure 6b).

4.2. Electricity production and CO_2 emission mitigation

This section assesses the utilization of the photovoltaic system, taking into account the ideal positioning determined before, to provide electricity to a standard building in Yazd, Iran. This evaluation aims to assess the influence of utilizing this electricity source on the mitigation of CO_2 emissions. By evaluation of the consumer electricity bills of Yazd in 2022, the average monthly consumption of a typical building is about 183.9 kWh, which is equivalent to 2206.8 kWh annually (Table 4).

Taking into account the findings of the prior section and assuming that all six modules of the photovoltaic system are operating at their peak levels, it is possible to supply the entire amount of elec-

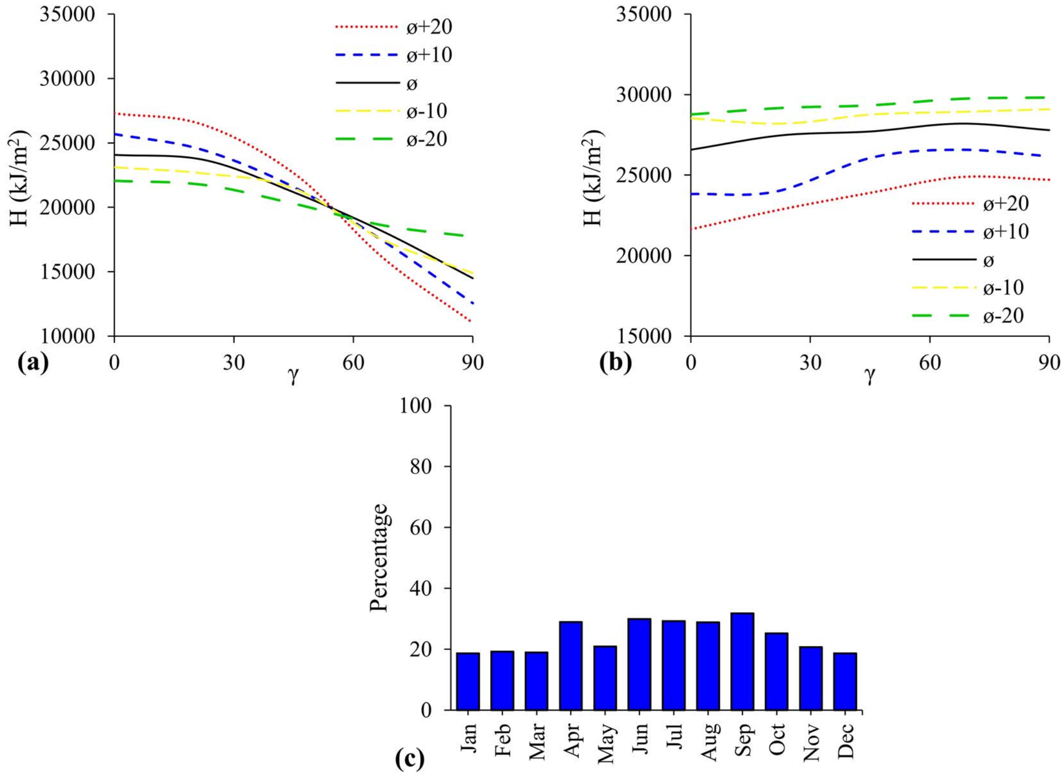

Figure 5. *The daily average total radiant energy reached the inclined surface for different azimuth angles in the months of (a) January, (b) July and (c) The attain energy receive in different mouths by optimal angel using the Klein model.*

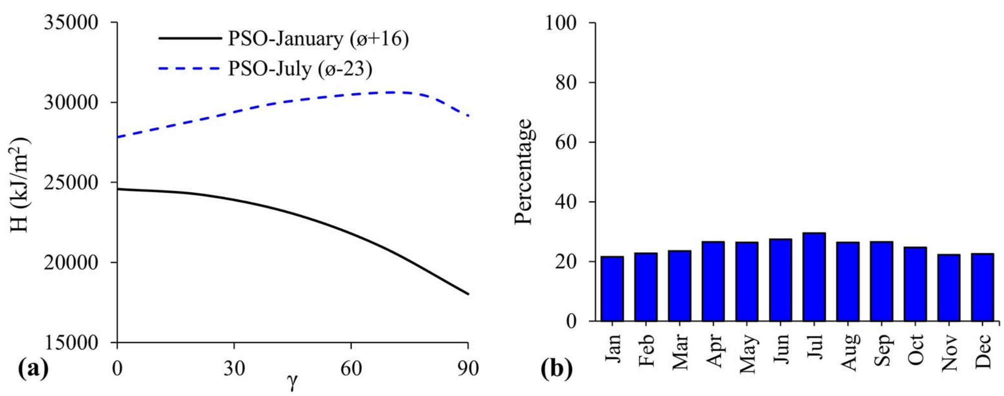

Figure 6. *(a) The daily average total radiant energy reached the inclined surface for different azimuth angles in the months of January and July (b) The attain energy receive in different mouths by optimal angel using PSO model.*

trical power required by the aforementioned building throughout the entire year. According to the findings of a study carried out by AlMallahi *et al*. [62], the production of a kilowatt-hour of electricity using a source of power other than renewable energy results in the release of ∼0.53 kg of CO_2 into the atmosphere. Figure 7 illustrates how the building in question has contributed to a lower overall level of CO_2 emissions into the atmosphere throughout the course of the year. Because this building unit makes optimal use of solar energy to produce electricity, the overall amount of CO_2 emissions that are released into the atmosphere is cut down by 1169.6 kg/year.

5. **Conclusions**

Solar panels are an extremely promising type of renewable energy technology for building energy supply. The optimal tilt angle is an important consideration when installing solar panels on building rooftops because it has a direct impact on the amount of energy generated annually, seasonally, monthly or daily. The effectiveness of the liquid that rises to the surface of the panels is notable. As demonstrated in this study, achieving maximum solar energy efficiency in a photovoltaic system requires optimizing solar panel orientation and collector angle in relation to sunlight. The goal of

Table 4. *Electricity load consumption in the studied building in Yazd, Iran in 2022*

Billing No	Billing period (days)	Total electrical load consumption (kWh)
1	57	129
2	62	502
3	63	589
4	61	567
5	61	302
6	61	118
Total	365	2207

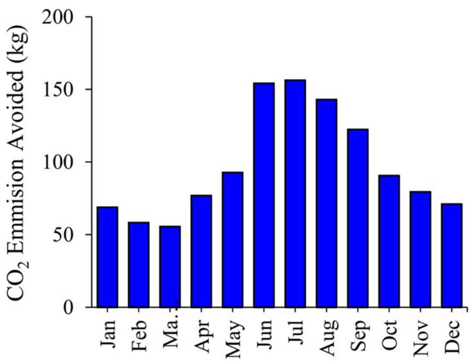

Figure 7. *CO_2 emission mitigation annually using optimal photovoltaic system in Yazd, Iran.*

this study is to determine the best inclination angle for solar panel collectors in a photovoltaic system designed for the urban region of Yazd, Iran. This will be accomplished by utilizing the isotropic, Kelin and PSO models.

The findings of the isotropic model from 2012 to 2022 show that the months of June and July have the highest daily, monthly and annual solar energy absorption. The city of Yazd in Iran receives the least amount of solar energy during the specified periods in January, as determined by its geographical location.

Klein's model suggests that for γ values less than 55, the angle of inclination is $\phi + 20$, which maximizes daily energy intake. When γ exceeds 55, the optimal inclination angle is $\phi - 20$. The results indicate that the model has the highest level of energy in July. The PSO algorithm produces the highest energy output in January at a slope angle of $\phi + 16$. Furthermore, the optimal azimuth angle for achieving the highest energy yield over the course of a year is determined to be 78. In June, the slope angle reaches its maximum potential energy output at $\phi - 23$. Furthermore, the ideal azimuth angle for maximizing energy absorption over the course of a year is zero. The optimal daily, monthly, seasonal and annual angles were used to calculate the received energy quantity.

The annual average solar energy quantities obtained using the optimal angles for isotropic, Kelin, and PSO models show a significant increase when compared to solar energy obtained at the horizon's surface. The percentage increases are 23.24, 24.47 and 25.02%, respectively. According to the results of an energy consumption analysis of a typical building in Yazd, using the optimal orientation for the photovoltaic power supply system can reduce the building's annual CO_2 emissions by 1169.6 kg.

Author contributions

Kairat A. Kuterbekov (Conceptualization [equal], Formal analysis [equal], Validation [equal], Visualization [equal]), Asset M. Kabyshev (Data curation [equal], Investigation [equal], Methodology [equal], Software [equal]), Kenzhebatyr Zh. Bekmyrza (Investigation [equal], Resources [equal], Software [equal], Visualization [equal], Writing—original draft [equal]), Marzhan M. Kubenova (Formal analysis [equal], Investigation [equal], Methodology [equal], Validation [equal]), and Abebe Ayalew (Investigation [equal], Visualization [equal], Writing – original draft [equal], Writing—review and editing [equal]).

Acknowledgements

The work was fulfilled in the frame of targeted financing program No. BR21882359, supported by the Ministry of Science and Higher Education of Kazakhstan.

REFERENCES

[1] Al-Aloosi W, Alaiwi Y, Hamzah H. Thermal performance analysis in a parabolic trough solar collector with a novel design of inserted fins. *Case Stud Therm Eng* 2023;**49**:103378. https://doi.org/10.1016/j.csite.2023.103378.

[2] Jasim MA, Ahmed OK, Alaiwi Y. Performance of solar stills integrated with PV/Thermal solar collectors: a review. *J Renew Energy* 2023;**4**:97–111. https://doi.org/10.56286/ntujre.v4i1.456.

[3] Molajou A, Afshar A, Khosravi M. *et al.* A new paradigm of water, food, and energy nexus. *Environ Sci Pollut Res* 2021;**30**:107487–97. https://doi.org/10.1007/s11356-021-13034-1.

[4] Molajou A, Pouladi P, Afshar A. Incorporating social system into water-food-energy nexus. *Water Resour Manag* 2021;**35**:4561–80. https://doi.org/10.1007/s11269-021-02967-4.

[5] Afshar A, Soleimanian E, Akbari Variani H. *et al.* The conceptual framework to determine interrelations and interactions for holistic Water, Energy, and Food Nexus. *Environ Dev Sustain* 2022;**24**:10119–40. https://doi.org/10.1007/s10668-021-01858-3.

[6] Puspitasari NB, Rosyada ZF, Habib FI. *et al.* The recommendations for implementation of green public procurement in hospitals. *Int J Ind Eng Manag* 2022;**13**:1–7. https://doi.org/10.24867/IJIEM-2022-1-296.

[7] Regina Moro S, Cauchick-Miguel PA, de Sousa-Zomer TT. *et al.* Design of a sustainable electric vehicle sharing business model in the Brazilian context. *Int J Ind Eng Manag* 2023;**14**:147–61. https://doi.org/10.24867/IJIEM-2023-2-330.

[8] Ahad A. Direct oral anticoagulants in the treatment of acute venous thromboembolism in patients with obesity: a systematic review with meta-analysis. *J Biomed Biochem* 2023;**2**:17–27. https://doi.org/10.57238/jbb.2023.6960.1038.

[9] Ali Abd Z, Jabbar N. Circulating Microrna-22 as a biomarker related to oxidative stress in hyperthyroid women patient. *J Biomed Biochem* 2023;**2**:28–37.

[10] Alobaidy Z, Alammar H, AL-harmooshee M. Evaluation of lipid profile, and preptin between obese non-diabetic patients and women with polycystic ovary syndrome in Al Diwaniyah, Iraq. *J Biomed Biochem* 2023;**2**:45–54. https://doi.org/10.57238/jbb.2023.7061.1045.

[11] Nejatian N, Abbaspour M, Javidan P. *et al.* Evaluation of the vulnerability and pathways of groundwater pollution in the Zanjanrud river basin by an integrated modeling approach. *Model Earth Syst Environ* 2023;**10**:2295–308. https://doi.org/10.1007/s40808-023-01897-x.
[12] Kong L, Wang L, Li F. *et al.* Life cycle-oriented low-carbon product design based on the constraint satisfaction problem. *Energy Convers Manag* 2023;**286**:117069. https://doi.org/10.1016/j.enconman.2023.117069.
[13] Luo J, Zhuo W, Liu S. *et al.* The optimization of carbon emission prediction in low carbon energy economy under big data. *IEEE Access* 2024;**12**:14690–702. https://doi.org/10.1109/ACCESS.2024.3351468.
[14] Zhang L, Yin Q, Zhu W. *et al.* Research on the orderly charging and discharging mechanism of electric vehicles considering travel characteristics and carbon quota. *IEEE Trans Transp Electrif* 2024;1–1. https://doi.org/10.1109/TTE.2023.3296964.
[15] Zhang L, Sun C, Cai G. *et al.* Charging and discharging optimization strategy for electric vehicles considering elasticity demand response. *ETransportation* 2023;**18**:100262. https://doi.org/10.1016/j.etran.2023.100262.
[16] Algarni S, Tirth V, Alqahtani T. *et al.* Contribution of renewable energy sources to the environmental impacts and economic benefits for sustainable development. *Sustain Energy Technol Assess* 2023;**56**:103098. https://doi.org/10.1016/j.seta.2023.103098.
[17] Teixeira JLV, Pinto FR. Solar panel: a sustainable development alternative for industries. *Int J Adv Eng Res Sci* 2020;**7**:160–3. https://doi.org/10.22161/ijaers.712.24.
[18] Mohamed MAS, Ibrahim AO, Bashir FM. *et al.* An assessment of the barriers to the adoption of green building technologies in Saudi Arabia. *Int J Low-Carbon Technol* 2023;**18**:872–80. https://doi.org/10.1093/ijlct/ctad064.
[19] Liu X, Liu X, Luo X. *et al.* Analysis of the influencing mechanism of command-and-control instruments on adopting energy consumption monitoring technology in public buildings. *Int J Low-Carbon Technol* 2020;**15**:210–23. https://doi.org/10.1093/ijlct/ctz075.
[20] Wang Z, Li J, Hu C. *et al.* Hybrid energy storage system and management strategy for motor drive with high torque overload. *J Energy Stor* 2024;**75**:109432. https://doi.org/10.1016/j.est.2023.109432.
[21] Meda US, Rajyaguru YV, Pandey A. Generation of green hydrogen using self-sustained regenerative fuel cells: Opportunities and challenges. *Int J Hydrog Energy* 2023;**48**:28289–314. https://doi.org/10.1016/j.ijhydene.2023.03.430.
[22] Wang Y, Qu K, Chen X. *et al.* Holistic electrification vs deep energy retrofits for optimal decarbonisation pathways of UK dwellings: a case study of the 1940s' British post-war masonry house. *Energy* 2022;**241**:122935. https://doi.org/10.1016/j.energy.2021.122935.
[23] Cuce PM, Saxena A, Cuce E. *et al.* Applications of solar PV tree systems with different design aspects and performance assessment. *Int J Low Carbon Technol* 2022;**17**:266–78. https://doi.org/10.1093/ijlct/ctac004.
[24] Cui Y, Theo E, Gurler T. *et al.* A comprehensive review on renewable and sustainable heating systems for poultry farming. *Int J Low Carbon Technol* 2020;**15**:121–42. https://doi.org/10.1093/ijlct/ctz048.
[25] Hayati MR, Ranjbar S, Abdar MR. *et al.* A comparative analysis of solar energy strategies in Middle East with rich fossil resources. *Iran J Energy Environ* 2023;**14**:271–88. https://doi.org/10.5829/IJEE.2023.14.03.09.
[26] Mohsen PS, Pourfayaz F, Shirmohammadia R. *et al.* Potential, current status, and applications of renewable energy in energy sector of iran: a review. *Renew Energy Res Appl* 2021;**2**:25–49. https://doi.org/10.22044/rera.2020.8841.1008.
[27] Hartmann H, Bastos A, Das AJ. *et al.* Climate change risks to global forest health: emergence of unexpected events of elevated tree mortality worldwide. *Annu Rev Plant Biol* 2022;**73**:673–702. https://doi.org/10.1146/annurev-arplant-102820-012804.
[28] Torres-Rivera AD, Mc Namara Valdes AJ, Florencio Da Silva R. The resilience of the renewable energy electromobility supply chain: review and trends. *Sustain For* 2023;**15**:10838. https://doi.org/10.3390/su151410838.
[29] Silber-Coats N. 2021. Zero Point Three. In Corva D, Meisel JS (eds). *The Routledge Handbook of Post-Prohibition Cannabis Research*. New York: Routledge. 201–15.
[30] Ahmed J, Bourazza S, Sarfraz M. *et al.* Heat transfer in Jeffrey fluid flow over a power law lubricated surface inspired by solar radiations and magnetic flux. *Case Stud Therm Eng* 2023;**49**:103220. https://doi.org/10.1016/j.csite.2023.103220.
[31] Obaideen K, Nooman AlMallahi M, Alami AH. *et al.* On the contribution of solar energy to sustainable developments goals: case study on Mohammed bin Rashid Al Maktoum Solar Park. *Int J Thermofluids* 2021;**12**:100123. https://doi.org/10.1016/j.ijft.2021.100123.
[32] Osman AI, Chen L, Yang M. *et al.* Cost, environmental impact, and resilience of renewable energy under a changing climate: a review. *Environ Chem Lett* 2023;**21**:741–64. https://doi.org/10.1007/s10311-022-01532-8.
[33] Liao C, Erbaugh JT, Kelly AC. *et al.* Clean energy transitions and human well-being outcomes in Lower and Middle Income Countries: a systematic review. *Renew Sust Energ Rev* 2021;**145**:111063. https://doi.org/10.1016/j.rser.2021.111063.
[34] Misbah Inayat S, Rafay Zaidi SM, Ahmed H. *et al.* Risk assessment and mitigation strategy of large-scale solar photovoltaic systems in Pakistan. *Int J Ind Eng Manag* 2023;**14**:105–21. https://doi.org/10.24867/IJIEM-2023-2-327.
[35] Taner T. A feasibility study of solar energy-techno economic analysis from Aksaray City, Turkey. *J Therm Eng* 2018;**5**:25–30. https://doi.org/10.18186/thermal.505498.
[36] Kumar D. 2023. Advancement in Renewable Energy Scenarios. In *Renewable Energy Scenarios in Future Indian Smart Cities. Advances in Geographical and Environmental Sciences*. Singapore: Springer. 37–89.
[37] Vokony I, Hartmann B, Talamon A. *et al.* On selecting optimum tilt angle for solar photovoltaic farms. *Int J Renew Energy Res* 2018;**8**:1926–35.
[38] Dogaheh ZR, Puig V. Tilt angle optimization of photovoltaic panels. *2019 6th International Conference on Control, Decision and Information Technologies (CoDIT), IEEE*; 2019, p. 1847–52.
[39] Kacira M, Simsek M, Babur Y. *et al.* Determining optimum tilt angles and orientations of photovoltaic panels in Sanliurfa, Turkey. *Renew Energy* 2004;**29**:1265–75. https://doi.org/10.1016/j.renene.2003.12.014.
[40] Almusaied Z, Asiabanpour B, Aslan S. Optimization of solar energy harvesting: an empirical approach. *J Solar Energy* 2018;**2018**:1–8. https://doi.org/10.1155/2018/9609735.
[41] Alfalari A, Alaiwi Y. Investigation of the effective factors on solar powered fixed-Wing UAV for extended flight endurance. *2022 International Symposium on Multidisciplinary Studies and Innovative Technologies (ISMSIT), IEEE*; 2022, p. 828–33.
[42] Liu Y, Liu X, Li X. *et al.* Model predictive control-based dual-mode operation of an energy-stored quasi-Z-source photovoltaic power system. *IEEE Trans Ind Electron* 2023;**70**:9169–80. https://doi.org/10.1109/TIE.2022.3215451.
[43] Li X, Aftab S, Hussain S. *et al.* Dimensional diversity (0D, 1D, 2D, and 3D) in perovskite solar cells: exploring the potential of mixed-dimensional integrations. *J Mater Chem A* 2024;**12**:4421–40. https://doi.org/10.1039/D3TA06953B.
[44] Yao L, Wang Y, Xiao X. Concentrated solar power plant modeling for power system studies. *IEEE Trans Power Syst* 2024;**39**:1–12.
[45] Benghanem M. Optimization of tilt angle for solar panel: case study for Madinah, Saudi Arabia. *Appl Energy* 2011;**88**:1427–33. https://doi.org/10.1016/j.apenergy.2010.10.001.
[46] Lahjouji D, Darhmaoui H. Tilt angle optimization for maximum solar energy collection - case study for Ifrane, Morocco. *2013 International Renewable and Sustainable Energy Conference (IRSEC), IEEE*; 2013, p. 96–101.
[47] Lubitz WD. Effect of manual tilt adjustments on incident irradiance on fixed and tracking solar panels. *Appl Energy* 2011;**88**:1710–9. https://doi.org/10.1016/j.apenergy.2010.11.008.
[48] Moghadam H, Tabrizi FF, Sharak AZ. Optimization of solar flat collector inclination. *Desalination* 2011;**265**:107–11. https://doi.org/10.1016/j.desal.2010.07.039.

[49] Lv Y, Si P, Rong X. *et al.* Determination of optimum tilt angle and orientation for solar collectors based on effective solar heat collection. *Appl Energy* 2018;**219**:11–9. https://doi.org/10.1016/j.apenergy.2018.03.014.

[50] Alharbi M, Alahmadi R, Alahmadi A. Meteorological-data-based modeling for PV performance optimization. *Sustain For* 2023;**15**:8659. https://doi.org/10.3390/su15118659.

[51] Al-Ghussain L, Taylan O, Abujubbeh M. *et al.* Optimizing the orientation of solar photovoltaic systems considering the effects of irradiation and cell temperature models with dust accumulation. *Sol Energy* 2023;**249**:67–80. https://doi.org/10.1016/j.solener.2022.11.029.

[52] Yoon S, Park J, Lee C. *et al.* Optimal Orientation of Solar Panels for Multi-Apartment Buildings. *Mathematics* 2023;**11**:938. https://doi.org/10.3390/math11040938.

[53] Liu B, Jordan R. Daily insolation on surfaces tilted towards the equator. *ASHRAE J* 1961;**3**:53–9.

[54] Orgill JF, Hollands KGT. Correlation equation for hourly diffuse radiation on a horizontal surface. *Sol Energy* 1977;**19**:357–9. https://doi.org/10.1016/0038-092X(77)90006-8.

[55] Klein SA. Calculation of monthly average insolation on tilted surfaces. *Sol Energy* 1977;**19**:325–9. https://doi.org/10.1016/0038-092X(77)90001-9.

[56] Zhang Z, Wu L, Wu Z. *et al.* Energy-saving oriented manufacturing workshop facility layout: a solution approach using multi-objective particle swarm optimization. *Sustain For* 2022;**14**:2788. https://doi.org/10.3390/su14052788.

[57] Elsheikh AH, Abd Elaziz M. Review on applications of particle swarm optimization in solar energy systems. *Int J Environ Sci Technol* 2019;**16**:1159–70. https://doi.org/10.1007/s13762-018-1970-x.

[58] Kuntoji G, Rao M, Rao S. Prediction of wave transmission over submerged reef of tandem breakwater using PSO-SVM and PSO-ANN techniques. *ISH J Hydraul Eng* 2020;**26**:283–90. https://doi.org/10.1080/09715010.2018.1482796.

[59] Rasheed M, Omar R, Sulaiman M. *et al.* Particle swarm optimisation (PSO) algorithm with reduced numberof switches in multilevel inverter (MLI). *Indones J Electr Eng Comput Sci* 2019;**14**:1114. https://doi.org/10.11591/ijeecs.v14.i3.pp1114-1124.

[60] Markvart T. *Solar Electricity, 2nd Edition. Synthesis Lectures on Power Electronics* 2000. John Wiley & Sons, England.

[61] Nijegorodov N, Adedoyin JA, Devan KRS. A new analytical-empirical model for the instantaneous diffuse radiation and experimental investigation of its validity. *Renew Energy* 1997;**11**:341–50. https://doi.org/10.1016/S0960-1481(96)00133-4.

[62] AlMallahi M, Nooman EH, Assad M. *et al.* Multi-criteria decision-making approach for the selection of cleaning method of solar PV panels in United Arab Emirates based on sustainability perspective. *Int J Low Carbon Technol* 2022;**17**:380–93. https://doi.org/10.1093/ijlct/ctac010.